Journal of Sound and Vibration 597 (2025) 118811

Contents lists available at ScienceDirect

Journal of Sound and Vibration

journal homepage: www.elsevier.com/locate/jsvi

# Assessing the quality of the time delay estimate in acoustic leak localisation

Ndubuisi Uchendu *, Jennifer M. Muggleton, Paul R. White

*Institute of Sound and Vibration Research (ISVR), University of Southampton, Southampton, SO17 1BJ, United Kingdom*

ARTICLE INFO

*Keywords:*
Leakage
Localisation
Time delay estimation
Cross-correlation function
Bayes factor
Peak-to-side lobe ratio
Peak-to-mean ratio

ABSTRACT

The problem considered in this paper is assessing the quality of the time delay estimate between leak signals measured on water pipes. This is practically important, as a quantitative assessment of the accuracy of time delay estimation (TDE) results makes it possible to infer the reliability of acoustic leak localisation results in a given situation. Three quality assessment approaches are developed by considering the statistical properties of the cross-correlation function (CCF): information-criterion, processing gain, and statistical approaches. In the information-criterion approach, the Bayes factor (BF) is employed to decide the most likely probability distribution of observed CCF peak values. The processing gain approach determines the quality of the time delay estimate using indices that indicate detectability of the CCF peak, namely, the peak-to-side lobe ratio (PSR) and the peak-to-mean ratio (PMR). In the statistical approach, an index termed inconsistency score (ICS) is used to describe the quality of TDE results based on root-mean square of deviations of time delay estimates from their statistical mode. Experimental results show that the proposed approaches provide effective means of assessing the accuracy of the time delay estimate in acoustic leak detection applications. Also, the proposed indices can be employed as figures of merit for selecting best parameters for TDE, for example, filter cut-off frequencies.

## 1. Introduction

Water pipelines are vital infrastructure for transporting water to consumers, and hence, are subject to high safety, integrity, and reliability requirements. The presence of leakages makes it difficult to satisfy these requirements [1]. Leakages can cause severe damage to the pipes and serve as potential entry points for contaminants, especially in low-pressure areas, thereby undermining the safety of water distribution networks. Loss of water through leakages decreases the reliability of pipelines and can lead to inability to meet demands. Lost revenue from leakages and cost of repair works place increased financial burden on water companies and may result in higher prices for the consumers. Dwindling freshwater supply and increasing threats of prolonged periods of drought make high prevalence of leakages a serious sustainability issue [2]. The global urban population facing water scarcity is projected to increase from 930 million in 2016 to 1.7–2.4 billion people in 2050 [3]. Due to the possibly disastrous consequences of water leakages, their timely detection and repair are of primal importance. Different leak detection methods have been developed, including use of listening sticks, fluid transient methods, optical fibre methods, pressure point analysis, acoustic methods [4].

Among the existing methods, acoustic cross-correlation using leak noise correlators provides a powerful solution for precisely locating a leak in water distribution networks [5]. In acoustic cross-correlation method, the leak location is determined from the time delay between acoustic/vibration signals acquired at two access points on either side of the suspected leak. Since this method

* Corresponding author.
*E-mail addresses:* n.uchendu@soton.ac.uk (N. Uchendu), jmm@isvr.soton.ac.uk (J.M. Muggleton), P.R.White@soton.ac.uk (P.R. White).

https://doi.org/10.1016/j.jsv.2024.118811
Received 23 April 2024; Received in revised form 25 October 2024; Accepted 29 October 2024

Available online 7 November 2024

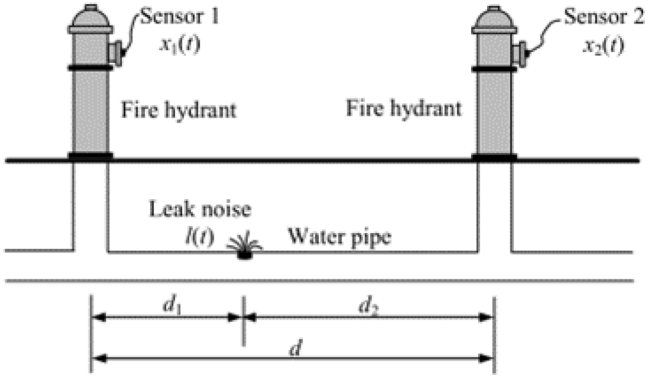


**Fig. 1.** Typical measurement setup for the acoustic cross-correlation method [9].

involves the classical time delay estimation (TDE) problem, it is difficult to make informed inferences about the reliability of leak localisation results without a quantitative assessment of the quality (accuracy) of the time delay estimate. However, this aspect of the TDE problem has not received widespread attention in the literature. Most of the existing research focuses mainly on improving TDE accuracy but fails to provide means for assessing the accuracy of the results. The few heuristic criteria available in the literature for assessing the quality of the time delay estimate include bandwidth-to-centre frequency ratio (BCFR) proposed in [6] and correlation quality index (CQI) proposed in [7]. The BCFR refers to the ratio of the bandwidth to centre frequency of the frequency band, over which the correlation analysis is carried out, while the CQI is the geometric mean of five component indices, namely, bandwidth index, coherence index, phase index, peak index, and shape index. The application of these indices is based on the observation that the time delay can be reliably determined when the cross-correlation function (CCF) has a 'good' shape characterised by a sharp and prominent main peak associated with the time delay and small correlation values away from this peak. Each index assesses the impact of different factors on the CCF shape: bandwidth of the leak signals (BCFR, bandwidth index); external noise (coherence index); noise, structural dynamics of the pipe system, and reflections (phase index, peak index); correlated noise and reflections (shape index). Certain drawbacks may render these indices ineffective for assessing the quality of the time delay estimate in some situations. Firstly, the indices consider only the CCF shape in inferring the quality of TDE results without taking into account the actual value of the time delay estimate. As a result, they are likely to provide incorrect inference about TDE quality in the presence of any factor that distorts the time delay estimate without changing the shape of the CCF, for example, when resonances are present in the analysed bandwidth [8]. Secondly, their usage is based on heuristic, non-rigorous considerations, leading to difficulties in setting appropriate thresholds and interpreting results. For instance, the shape index attains a high value for CCF of uncorrelated signals and CCF of leak signals with a 'good' shape, making it difficult to distinguish between these two cases. Also, the phase index may attain a negative value, interpretation of which is unclear. Thirdly, some of the indices included in the CQI are cumbersome to calculate. An example is the phase index, which requires linear regression.

This paper addresses the research gap concerning lack of adequate and robust indices for assessing the accuracy of the time delay estimate between measured leak signals. In this work, alternative quality assessment indices based on three different approaches are developed by considering the properties of the CCF relevant for TDE. In the first approach, the quality of the time delay estimate is assessed using an information criterion that describes the statistical distribution of the CCF peak value. The second approach termed the processing gain approach infers the quality of TDE results based on the prominence of the CCF peak. In the third approach, the root-mean square of deviations of time delay estimates from their statistical mode is used to quantify TDE accuracy. Experimental signals are used to investigate and compare the effectiveness of the proposed indices. The outline of the paper is as follows. Section 2 gives an overview of the acoustic cross-correlation technique and illustrates the impact of TDE errors on leak localisation results. Indices for quality assessment of TDE results are proposed in Section 3. Experimental results are presented and discussed in Section 4, while the main findings are summarised in Section 5.

## 2. Overview of acoustic cross-correlation

Fig. 1 shows the typical measurement setup used to detect and locate leaks in water pipes. Acoustic/vibration sensors are attached to access points, typically hydrants or valves, on either side of the suspected leak. In the cross-correlation method, the distance $d_1$ between the leak and the first measurement point is calculated as [9]

$$d_1 = \frac{d - c \cdot \tau_{\text{peak}}}{2} \tag{1}$$

where $c$ is the acoustic wave speed in the pipe, $d = d_1 + d_2$ is the distance between the measurement points, and $\tau_{\text{peak}} = (d_2 - d_1)/c$ is the time delay between the measured signals. In leak noise correlators, $\tau_{\text{peak}}$ is usually estimated as the lag corresponding to the peak of the CCF of the measured signals.

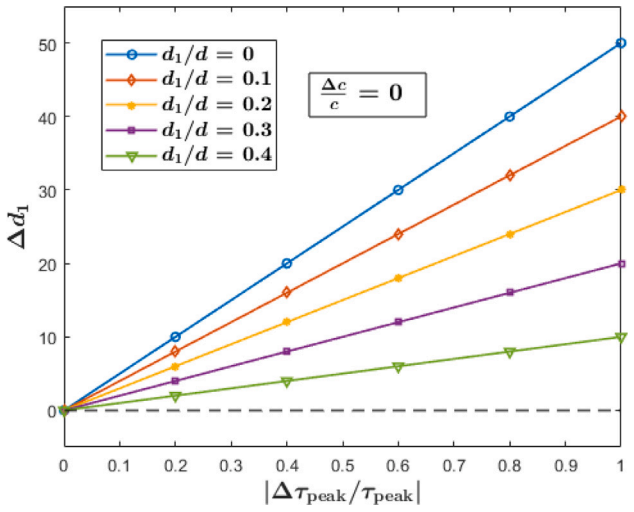


**Fig. 2.** Absolute leak localisation error due to TDE error for different relative leak locations.

For accurate determination of the leak location, accurate estimates of $c$ and $\tau_{\text{peak}}$ are required. An error in either of these quantities will produce a corresponding error in the estimate of $d_1$. Let $\hat{d}_1$ denote the leak location calculated using the time delay estimate $\hat{\tau}_{\text{peak}}$ and some wave speed value $\hat{c}$ in Eq. (1). Denoting $\Delta\tau_{\text{peak}} = \hat{\tau}_{\text{peak}} - \tau_{\text{peak}}$ and $\Delta c = \hat{c} - c$, the absolute error in leak location $\Delta d_1 = |\hat{d}_1 - d_1|$ is given by

$$\begin{aligned}\Delta d_1 &= \frac{1}{2}\left|\tau_{\text{peak}}\cdot\Delta c + c\cdot\Delta\tau_{\text{peak}} + \Delta c\cdot\Delta\tau_{\text{peak}}\right| \\ &= \left|d\cdot\left(\frac{1}{2}-\frac{d_1}{d}\right)\left(\frac{\Delta c}{c}+\frac{\Delta\hat{\tau}_{\text{peak}}}{\tau_{\text{peak}}}\right)+\frac{\Delta c\cdot\Delta\tau_{\text{peak}}}{2}\right| \\ &= \frac{c\cdot\tau_{\text{peak}}}{2}\left|\left(\frac{\Delta\tau_{\text{peak}}}{\tau_{\text{peak}}}+1\right)\left(\frac{\Delta c}{c}+1\right)-1\right|.\end{aligned} \tag{2}$$

The last two expressions in Eq. (2) are only valid for $\tau_{\text{peak}} \neq 0$, i.e., when the leak is not exactly at the midpoint of the pipe. It can be observed that even when the wave speed or time delay is exactly known, leak localisation error due to error in the other can be large especially if the true leak location is closer to one end of the pipe. Fig. 2 shows the absolute leak localisation error due to error in the time delay estimate for different locations of the leak when $d = 100$ m, $c = 354$ m/s, and $\Delta c = 0$. For $d_1/d = 0.2$, a 10% error in the time delay estimate will result in an undesirable absolute leak localisation error of $|\Delta d_1| = 3$ m. Since error in the time delay estimate has a substantial effect on acoustic leak localisation results, assessing its accuracy is of practical importance. As stated in the introduction, BCFR and CQI were proposed for assessment of the quality of the time delay estimate. The BCFR can be calculated from the CCF of the signals as [6]

$$\text{BCFR} \approx \frac{1}{\pi}\sqrt{6(1-\alpha)} \tag{3}$$

where $\alpha$ is the ratio of the heights of the adjacent and main peaks in the CCF envelope. The CQI is given by [7]

$$\text{CQI} = \sqrt[5]{k_{\text{b}}k_{\text{co}}k_{\text{ph}}k_{\text{pk}}k_{\text{sh}}} \tag{4}$$

where $k_{\text{b}} = 1 - \widehat{R}_2$ is the bandwidth index, $k_{\text{co}} = \frac{1}{N_f}\sum_{i=1}^{N_f-1}\gamma^2_{x_1x_2}(\omega_i)$ is the coherence index, $k_{\text{ph}} = 1 - \sqrt{\frac{1}{N_f-1}\sum\left(\left|r_{\text{ph}}-1\right|-\mu\right)^2}$ is the phase index, $k_{\text{pk}} = \max\{\rho_{x_1x_2}(\tau)\}$ is the peak index, and $k_{\text{sh}} = 1 - R_2$ is the shape index. Here, $\max\{\cdot\}$ represents the maximum value, $\widehat{R}_2$ denotes the second highest peak in the CCF envelope, $\rho_{x_1x_2}(\tau)$ is the normalised CCF, $R_2$ is the height of the second highest (secondary) peak in the CCF, $r_{\text{ph}}$ is the ratio between the experimental unwrapped cross-spectral phase to its least squares fit, $\mu$ is the mean of $|r_{\text{ph}} - 1|$, $\omega_i$ is the $i$th frequency in the frequency band over which the leak noise propagates, and $N_f$ is the number of frequency points. These indices assess the CCF shape in terms of how prominent the main peak is relative to other CCF values. Large values imply that the CCF has a 'good' shape desirable for accurate TDE results. On the other hand, low values indicate CCF with a 'bad' shape, in which the main peak may be of comparable height with other peaks, thus making it difficult to unambiguously identify the time delay. The following scale for inferring the quality of time delay estimates was suggested in [7]: CQI values 0–0.2 denote poor quality, 0.2–0.7 good quality, and 0.7–1.0 excellent quality. Values of BCFR above 0.3 indicate accurate time delay estimates [6]. These indices may not be effective and robust due to the drawbacks highlighted in the introduction. Developing more effective quality assessment indices is the main motivation for the work in this paper.

## 3. Approaches for assessing quality of the time delay estimate

Since time delay between leak signals is usually estimated using a correlation-based method, this paper will focus only on assessing the quality of time delay estimates obtained from the peak of the CCF. Referring to Fig. 1, the measured signals $x_1(t)$ and $x_2(t)$ can be represented as

$$x_1(t) = l(t) \otimes h_1(t) + n_1(t) = l_1(t) + n_1(t) \tag{5a}$$

$$x_2(t) = l(t) \otimes h_2(t) + n_2(t) = l_2(t) + n_2(t) \tag{5b}$$

where $l(t)$ is the signal generated at the leak location (i.e., the leak noise), $h_i$, $i = 1, 2$, is the impulse response function (IRF) that expresses the relationship between $l(t)$ and the signal at the $i$th measurement point, $l_i = l(t) \otimes h_i$ is the noise-free component of $x_i(t)$, and $n_i(t)$ is the background noise, which is assumed to be uncorrelated with the leak noise. For an infinitely long pipe without discontinuities, the frequency response function (FRF) $H(\omega, d_i) = \mathcal{F}\left\{h_i\right\}$ has the following form [9]

$$H(\omega, d_i) = \exp(-|\omega|\beta d_i) \cdot \exp(-\mathrm{j}|\omega| d_i / c) \tag{6}$$

where $\beta$ is the attenuation factor (a measure of the loss experienced by acoustic waves within the pipe wall), $\omega$ is the radial frequency, $\mathrm{j} = \sqrt{-1}$, and $\mathcal{F}\{\bullet\}$ denotes the Fourier transform (FT). The CCF $R_{x_1x_2}(\tau)$ of the leak signals $x_1(t)$ and $x_2(t)$ can be expressed as

$$R_{x_1x_2}(\tau) = R_{l_1l_2}(\tau) + R_{l_1n_2}(\tau) + R_{n_1l_2}(\tau) + R_{n_1n_2}(\tau) \tag{7}$$

where $R_{uv}(\tau) = \frac{1}{T}\int_0^T u(t+\tau)v(t)dt$ is the CCF of signals $u$ and $v$ [10], and $T$ is the measurement time.

Reliable TDE and leak localisation can only be accomplished when a distinct peak can be identified in the CCF. Since the leak noise and background noise signals are assumed to be mutually uncorrelated, a distinct peak will only be observed in the CCF when there is 'strong' correlation between the measured leak signals. 'Poor' correlation due to noise and severe signal attenuation makes it difficult to correctly identify the time delay from the CCF. High background noise level and interferences, such as reflections and resonances, increase the 'background' correlation values (i.e., CCF values away from the main peak) and induce additional peaks in the CCF, while signal attenuation broadens and reduces the main CCF peak [9]. In this paper, the term 'poor correlation' is used to indicate that the leak signal level is so low such that noise dominates in the measured signals, while 'strong correlation' implies the contrary. Examples of CCFs of poorly and strongly correlated signals are shown in Figs. 3(a) and 3(b). Assessing the quality of the time delay estimate can be essentially considered a binary hypothesis problem, the aim of which is to infer whether the measured signals are strongly or poorly correlated. In practical applications, the true delay is not known a priori, so the quality of the time delay estimate can only be assessed indirectly by considering the properties of the CCF relevant for TDE, namely, the location $\tau = \tau_{\text{peak}}$ and the value $R_{\max}$ of the main peak. The former gives the time delay estimate, while the latter affects the ability to unambiguously determine this estimate. To facilitate development of indices for assessing the quality of the time delay estimate, these properties are considered for strongly and poorly correlated signals.

### 3.1. Information criterion approach

The information criterion approach is based on the statistical distribution of the CCF peak value. It can be shown that $R_{\max}$ follows different distributions depending on whether the measured signals are strongly or poorly correlated.

#### 3.1.1. Distribution of the CCF peak value

The case of poor correlation is first considered. According to the central limit theorem, the cross-correlation values $R_{n_1n_2}(\tau)$ of zero-mean signals $n_1(t)$ and $n_2(t)$ is normally distributed with zero mean and variance $\frac{\sigma_{n_1}^2\sigma_{n_2}^2}{N}$, where $\sigma_u^2$ denotes the variance of $u$ and $N$ is the signal length [11,12]. This is denoted as $R_{n_1n_2}(\tau) \sim \mathcal{N}\left(0, \frac{\sigma_{n_1}^2\sigma_{n_2}^2}{N}\right)$. Based on the extreme value theorem, $R_{\max} = \max\{R_{n_1n_2}(\tau)\}$ is distributed according to a type I generalised extreme value (GEV) or Gumbel distribution with a null shape parameter, location parameter $\mu_Y(N_c)$, and scale parameter $s_Y(N_c)$ given by [13].

$$\mu_Y(N_c) = Y^{-1}\left(1 - \frac{1}{N_c}\right) \tag{8a}$$

$$s_Y(N_c) = Y^{-1}\left(1 - \frac{1}{N_c \cdot \mathrm{e}}\right) - Y^{-1}\left(1 - \frac{1}{N_c}\right) \tag{8b}$$

where $N_c$ is the CCF size (number of lags in the CCF), and $Y^{-1}(\bullet)$ is the inverse of the cumulative distribution function (CDF) $Y(\bullet)$ of $R_{n_1n_2}(\tau)$. This is denoted as $R_{\max} \sim \mathrm{GEV}_1(\mu_Y(N_c), s_Y(N_c))$.

The CCF $R_{x_1x_2}(\tau)$ in Eq. (7) is the sum of the term $R_{l_1l_2}(\tau)$ and the noise terms $R_N(\tau) = R_{l_1n_2}(\tau) + R_{n_1l_2}(\tau) + R_{n_1n_2}(\tau)$. The value of $R_{l_1l_2}(\tau_{\text{peak}})$ over multiple realisations of the CCF of strongly correlated leak signals can be assumed to be approximately constant since it is not affected by noise. Note that this assumption is not strictly true since $R_{l_1l_2}(\tau_{\text{peak}})$ depends on the leak noise $l(t)$, a random signal. The term $R_N(\tau)$ is the sum of three normally distributed zero-mean random variables (CCFs of uncorrelated signals). Hence, the distribution of $R_{\max}$ in the case of strongly correlated leak signals is a normal distribution with mean $\mu_{R_{\max}} = R_{l_1l_2}(\tau_{\text{peak}})$ and variance $\sigma_{R_{\max}}^2 = \frac{1}{N}\left(\sigma_{l_1}^2\sigma_{n_2}^2 + \sigma_{n_1}^2\sigma_{l_2}^2 + \sigma_{n_1}^2\sigma_{n_2}^2\right)$, i.e., $R_{\max} \sim \mathcal{N}\left(\mu_{R_{\max}}, \sigma_{R_{\max}}^2\right)$.

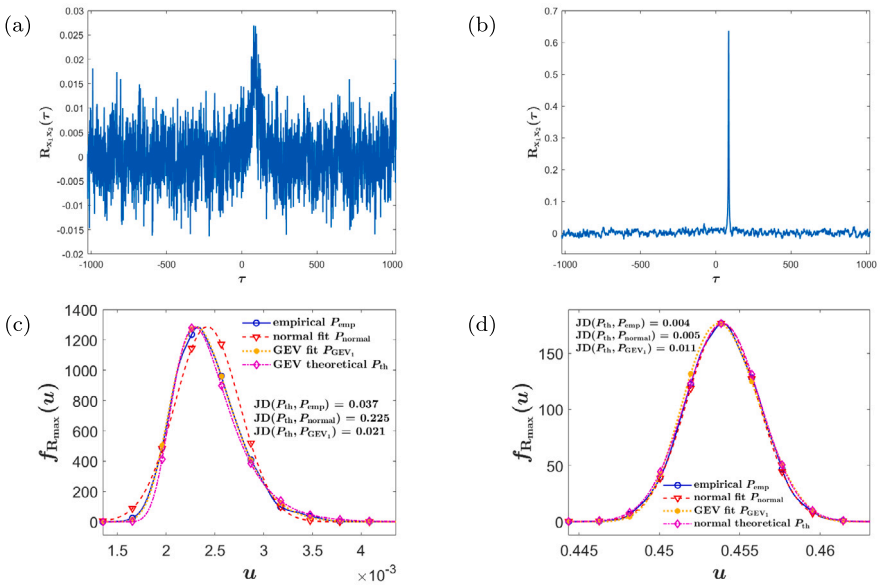


**Fig. 3.** Examples of CCFs of (a) poorly correlated leak signals and (b) strongly correlated leak signals. Comparison of GEV and normal distributions for describing the PDF of the CCF peak in the case of: (c) poorly correlated leak signals; (d) strongly correlated leak signals.

Figs. 3(c) and 3(d) show the empirical probability distribution functions (PDFs) of $R_{\max}$ for strongly correlated and poorly correlated simulated leak signals, respectively. The strongly correlated leak signals were obtained by filtering the white noise signal with the FRFs (Eq. (6)) of a pipe with the following properties: wave speed $c = 354$ m/s, relatively small attenuation factor $\beta = 2.1 \cdot 10^{-5}$ s/m, $d_1 = 20$ m, and $d_2 = 50$ m. To obtain poorly correlated leak signals, the pipe attenuation factor was increased to $\beta = 2.1 \cdot 10^{-3}$, and white Gaussian noise was added such that the signal-to-noise ratio (SNR) of the resulting signals was −7 dB. Also shown on Figs. 3(c) and 3(d) are the PDFs of the theoretical distributions $\text{GEV}_1(\mu_Y(N), s_Y(N))$ and $\mathcal{N}\left(\mu_{R_{\max}}, \sigma^2_{R_{\max}}\right)$, respectively, as well as the fitted GEV and normal distributions. In the figures, the empirical and the theoretical PDFs are denoted as $P_{\text{emp}}$ and $P_{\text{th}}$, respectively, while the fitted normal and GEV PDFs are denoted as $P_{\text{normal}}$ and $P_{\text{GEV}_1}$, respectively. The empirical PDFs were estimated using the MATLAB density estimation function 'ksdensity', while the fitted PDFs were obtained using the MATLAB distribution fitting function 'fistdist' with the desired distribution (GEV or normal) specified. The relative agreement between these PDFs can be objectively assessed using Jeffrey's divergence (JD), which for two probability distributions $P$ and $Q$ defined in the same sample space $\mathcal{X}$ is given by [14]

$$\text{JD}(P, Q) = \sum_{u \in \mathcal{X}} (P(u) - Q(u)) \cdot \log\left\{\frac{P(u)}{Q(u)}\right\}. \tag{9}$$

A small JD implies high similarity between the distributions, while a high JD indicates that the distributions are very different. Based on the JD values, $R_{\max}$ is best described by different distributions as predicted above: GEV for poorly correlated leak signals and normal for strongly correlated leak signals. However, the extent to which the distributions best describe $R_{\max}$ in each case differs. By visual inspection and from the relatively high value of $\text{JD}(P_{\text{th}}, P_{\text{normal}})$ in Fig. 3(c), the normal distribution is a rather poor fit for $R_{\max}$ in the case of poorly correlated signals. On the other hand, while the normal distribution is objectively the better fit in the case of strongly correlated leak signals, the GEV appears to be a good fit in some regions, as shown by the relatively small value of $\text{JD}(P_{\text{th}}, P_{\text{GEV}_1})$ in Fig. 3(d).

### 3.1.2. *Bayes factor as a quality assessment index*

Since $R_{\max}$ follows different distributions depending on the strength of correlation between the measured leak signals, the problem of assessing the quality of the time delay estimate can be considered a model selection problem, or more specifically, the problem of deciding whether the observed CCF peak values are best described by a type I GEV distribution (denoted as $M_1$) or a normal distribution (denoted as $M_2$). Information criteria, such as the Bayes factor (BF), are widely employed in such model discrimination problems. The BF of two candidate models is defined as the ratio of their marginal likelihoods, i.e., the likelihoods of the two models integrated over the prior probabilities of their parameters [15]. For a large sample size, the BF $\text{BF}_{M_1,M_2}$ of models $M_1$ and $M_2$ can be approximated as [16]

$$\text{BF}_{M_1,M_2} = \exp\left\{-\frac{\text{BIC}_{M_1} - \text{BIC}_{M_2}}{2}\right\} \tag{10}$$

**Table 1**
Scales for the interpretation of the BF.

| $\log_{10}(\mathrm{BF}_{M_1,M_2})$ | $\mathrm{BF}_{M_1,M_2}$ | Strength of evidence in support of $M_1$ | |
|---|---|---|---|
| | | Kass and Raftery (1995) | Jeffreys (1998) |
| <0 | <1 | Negative (supports $M_2$) | |
| 0 to 1/2 | 1 to 3.2 | Barely worth mentioning | |
| 1/2 to 1 | 3.2 to 10 | Substantial | Substantial |
| 1 to 3/2 | 10 to 31.6 | Strong | Strong |
| 3/2 to 2 | 31.6 to 100 | | Very strong |
| >2 | >100 | Decisive | |

where $\mathrm{BIC}_{M_i}$ is the Bayesian Information Criterion (BIC) of model $M_i$, $i = 1, 2$, given by [17]

$$\mathrm{BIC}_{M_i} = k \log\left(N_R\right) - 2\log\left(L_{M_i}\right) \tag{11}$$

where $L_{M_i}$ is the maximised value of the likelihood function of $M_i$, i.e., $L_{M_i} = \Pr\left\{\hat{R}_{\max} \middle| \hat{\theta}, M_i\right\}$, $\hat{\theta}$ are the parameter values that maximise the likelihood function, $\hat{R}_{\max}$ is the observed CCF peak data, $N_R$ is the sample size (number of CCF peak values), and $k$ is the number of parameters in the model distribution $M_i$. A value of $\mathrm{BF}_{M_1,M_2} > 1$ implies that $M_1$ is more strongly supported by the data under consideration than $M_2$. Two scales proposed by Kass and Raftery [18] and Jeffreys [14] for the interpretation of the BF are shown in Table 1. In both scales, inference is made in favour of $M_1$ only if there is at least a substantial evidence in support of $M_1$. Otherwise, it is decided in favour of $M_2$. Based on this, the time delay estimate is considered accurate if $\mathrm{BF}_{M_1,M_2} \geq 3.2$ and inaccurate otherwise. Note that the inference has been formulated as accepting or rejecting the hypothesis that $R_{\max}$ follows a GEV distribution. This is because as illustrated above, difficulty may arise in distinguishing between normal and GEV distributions for CCF peak value of strongly correlated signals. Conversely, a substantial evidence in support of GEV distribution ($M_1$) is expected when the signals are poorly correlated.

### 3.2. Processing gain approach

A parameter used for assessing the performance of a signal processor is the signal-to-noise (SNR) $\mathrm{SNR}_{\mathrm{out}}$ of its output [19]. Given the same input signals, signal processors with higher output SNR are generally more robust to noise and other factors that may negatively impact performance. For a correlation-based time delay estimator, $\mathrm{SNR}_{\mathrm{out}}$ is essentially the SNR of the CCF, which can be defined as the ratio of a 'useful' component to a 'noise' component in the CCF. Here, a 'useful' component denotes the part of the CCF that contains information about the time delay (for example, the CCF peak height), while the 'noise components' refer to CCF components that interfere with the ability to unambiguously determine the time delay (for example, CCF values away from the main peak). Two indices based on this definition of $\mathrm{SNR}_{\mathrm{out}}$ are described in the following subsections.

#### 3.2.1. Peak-to-side lobe ratio as a quality assessment index

The SNR of the CCF can be expressed as the peak-to-side lobe ratio (PSR), which is defined as

$$\mathrm{SNR}_{\mathrm{out}} = \mathrm{PSR} = \frac{R^2_{x_1x_2}(\tau_{\mathrm{peak}})}{\mathrm{var}\left\{R_{x_1x_2}(\tau_{\mathrm{far}})\right\}} \tag{12}$$

where $\mathrm{var}\left\{R_{x_1x_2}(\tau_{\mathrm{far}})\right\}$ denotes the variance of the CCF 'side lobe'. Here, 'side lobe' refers to the 'background' CCF values at lags $\tau_{\mathrm{far}}$ *far away* from the main CCF peak. If the CCF is computed in the lag interval $-n_c \leq \tau \leq n_c$, then $\tau_{\mathrm{far}}$ encompasses lags at least $n_c/2$ away from $\tau_{\mathrm{peak}}$. The PSR can be considered a quantitative measure of peak detectability with a higher value indicating a CCF with a prominent peak and low values off from this peak, which is desirable for accurate TDE. A low PSR value implies a less prominent main peak in the CCF. In this sense, it characterises the CCF shape like the BCFR.

The PSR can be expressed analytically. Since $R_{n_1n_2}(\tau) \sim \mathcal{N}\left(0, \frac{\sigma^2_{n_1}\sigma^2_{n_2}}{N}\right)$, the quantity $\dfrac{R_{n_1n_2}(\tau)}{\sqrt{\mathrm{var}\left\{R_{n_1n_2}(\tau)\right\}}} \sim \mathcal{N}(0,1)$, i.e., a standard normal random variable. Thus, in the case of poorly correlated signals, the square root of the PSR follows a type I GEV distribution; specifically, $\sqrt{\mathrm{PSR}} \sim \mathrm{GEV}_1\left(\mu_{\Phi}(N_c), s_{\Phi}(N_c)\right)$, where $\mu_{\Phi}(N_c)$ and $s_{\Phi}(N_c)$ are evaluated using Eq. (8) with $\Phi(\bullet)$ the standard normal CDF. The expected value of the PSR for such signals can thus be expressed as [13]

$$\begin{aligned}\mathrm{PSR} &= \left[\mu_{\Phi}(N_c) + \gamma \cdot s_{\Phi}(N_c)\right]^2 \\ &= \left[(1-\gamma)\Phi^{-1}\left(1 - \frac{1}{N_c}\right) + \gamma \cdot \Phi^{-1}\left(1 - \frac{1}{N_c \cdot \mathrm{e}}\right)\right]^2\end{aligned} \tag{13}$$

where $\gamma = 0.5772$ is the Euler–Mascheroni constant.

In the case of strongly correlated signals, the square root of the PSR is normally distributed, and the PSR can be expressed as (Appendix)

$$\mathrm{PSR} = \frac{T}{\pi(\beta d)^2}\left[\begin{array}{l}\dfrac{1}{2\beta d}\exp(-2\omega_1\beta d)\displaystyle\sum_{k=0}^{2}\frac{(2\omega_1\beta d)^k}{k!} + \frac{N_0}{S_0}\frac{1}{2\beta d_1}\exp(-2\omega_1\beta d_1)\sum_{k=0}^{2}\frac{(2\omega_1\beta d_1)^k}{k!} \\ +\dfrac{N_0}{S_0}\dfrac{1}{2\beta d_2}\exp(-2\omega_1\beta d_2)\displaystyle\sum_{k=0}^{2}\frac{(2\omega_1\beta d_2)^k}{k!} + \frac{N_0^2}{S_0^2}\omega_2\end{array}\right]^{-1} \tag{14}$$

where flat spectra $G_{ll}(\omega) = S_0$ and $G_{n_1n_1}(\omega) = G_{n_2n_2}(\omega) = N_0$ have been assumed for the leak noise and background noise signals in the analysed frequency region $\omega_1 \le \omega \le \omega_2$ with $\omega_2 \gg \omega_1$. From this expression, it can be observed that the PSR of leak signals attains a higher value in situations where the accuracy of the time delay estimate is expected to be higher: lower pipe attenuation factor $\beta$, smaller inter-sensor distance $d$, longer measurement duration $T$, and larger ratio of the powers of the leak noise and background noise $S_0/N_0$.

Inference about the quality of the time delay estimate is made by comparing the PSR value to a threshold $\lambda_{\mathrm{PSR}}$ that can be set using the common approach in binary hypothesis testing as

$$\lambda_{\mathrm{PSR}} = \left[F^{-1}_{\sqrt{\mathrm{PSR}}}(1-\xi)\right]^2 \tag{15}$$

where $F^{-1}_{\sqrt{\mathrm{PSR}}}(\bullet)$ is the inverse of the CDF of the type I GEV distribution $\mathrm{GEV}_1\left(\mu_{\boldsymbol{\Phi}}(N_c), s_{\boldsymbol{\Phi}}(N_c)\right)$, and $\xi$ is the allowable false positive rate (AFPR), which denotes the probability that PSR exceeds $\lambda_{\mathrm{PSR}}$ for poorly correlated signals. If the PSR exceeds $\lambda_{\mathrm{PSR}}$, then it is inferred that the time delay estimate provided by the CCF is accurate. Otherwise, the estimate is considered inaccurate.

### 3.2.2. Peak-to-mean ratio as a quality assessment index

An alternative way to define the SNR of the CCF is in terms of the mean of the correlation values as the peak-to-mean ratio (PMR) given by

$$\mathrm{PMR} = \frac{R_{\max}}{\frac{1}{N_c}\sum|R_{x_1x_2}(\tau)|}. \tag{16}$$

The PMR describes how much the CCF peak 'sticks out' above the CCF mean level. It is a heuristic measure used in the water industry to infer reliability of cross-correlation results. For the background noise signals $n_1(t)$ and $n_2(t)$, the absolute value $\left|R_{n_1n_2}(\tau)\right|$ follows a folded normal distribution [20] with mean $\sqrt{\dfrac{2\sigma_{n_1}^2\sigma_{n_2}^2}{\pi N}}$ and variance $\dfrac{(1-\frac{2}{\pi})\cdot\sigma_{n_1}^2\sigma_{n_2}^2}{N}$. Therefore, according to the central limit theorem, provided $N_c$ is large, the quantity $\kappa(\tau) = \dfrac{R_{n_1n_2}(\tau)}{\frac{1}{N_c}\sum|R_{x_1x_2}(\tau)|} \sim \mathcal{N}(0,\pi/2)$. From this, it follows that $\mathrm{PMR} \sim \mathrm{GEV}_1\left(\mu_{F_\kappa}(N_c), s_{F_\kappa}(N_c)\right)$, where $\mu_{F_\kappa}(N_c)$ and $s_{F_\kappa}(N_c)$ are evaluated using Eq. (8) with $F_\kappa(u) = \boldsymbol{\Phi}\left(\dfrac{u}{\sqrt{\pi/2}}\right)$. Thus, when the signals are poorly correlated, the expected value of the PMR can be expressed as [13]

$$\begin{aligned}\mathrm{PMR} =& \mu_{F_\kappa}(N_c) + \gamma\cdot s_{F_\kappa}(N_c) \\ =& \left[(1-\gamma)\boldsymbol{\Phi}^{-1}\left(1-\frac{1}{N_c}\right) + \gamma\cdot\boldsymbol{\Phi}^{-1}\left(1-\frac{1}{N_c\cdot\mathrm{e}}\right)\right]\cdot\sqrt{\frac{\pi}{2}}.\end{aligned} \tag{17}$$

Comparison of Eqs. (13) and (17) shows that the PMR and PSR are closely related. The PSR is the squared value of the PMR scaled by a factor of $\pi/2$.

In the case of strongly correlated leak signals, the PMR cannot be expressed analytically since there is no closed form expression for the absolute correlation value $\left|R_{x_1x_2}(\tau)\right|$. However, it can be easily observed that like the square root of the PSR, the PMR of leak signals will be normally distributed in this case.

Following the same procedures employed for the PSR, accurate time delay estimate is inferred if the PMR exceeds a threshold $\lambda_{\mathrm{PMR}}$ given by

$$\lambda_{\mathrm{PMR}} = F^{-1}_{\mathrm{PMR}}(1-\xi) \tag{18}$$

where $F^{-1}_{\mathrm{PMR}}(\bullet)$ is the inverse of the CDF of the type I GEV distribution $\mathrm{GEV}_1\left(\mu_{F_\kappa}(N_c), s_{F_\kappa}(N_c)\right)$. Compared to BCFR and CQI thresholds, which are set arbitrarily, the PSR and PMR thresholds defined in Eqs. (15) and (18) are likely to be more robust and reduce incidents of false alarms (i.e., incorrectly inferring strong correlation when there is none).

### 3.3. Statistical approach

One issue with the information criterion and processing gain approaches described above is that they do not explicitly take the actual value of the time delay estimate into account. To deal with this issue, an additional quality assessment index, referred to as the inconsistency score (ICS) and denoted as $C_s$ in this paper, is proposed as follows:

$$C_s = \sqrt{\frac{1}{N_R}\sum_{k=1}^{N_R}\left(\hat{\tau}_{\text{peak},i} - \tilde{\tau}_{\text{peak}}\right)^2} \tag{19}$$

where $N_R$ is the number of CCF realisations (obtained from signal segments or multiple measurements from the same leak), $\hat{\tau}_{\text{peak},i}$ is the time delay estimate from the $i$th CCF realisation, and $\tilde{\tau}_{\text{peak}}$ is the *assumed* true delay taken as the statistical mode of the time delay estimates. Here, the term *assumed* is used to emphasise that the true delay is not known a priori. The ICS is similar to the standard deviation but defined in terms of the mode instead of the mean. A justification for the choice of the statistical mode over the statistical mean in the definition of the ICS is that the effects of outliers are less pronounced on the mode. In this work, a time delay estimate is said to be *inconsistent* if it differs from the assumed true time delay by more than some given value. The ICS assesses the *inconsistency* of time delay estimates obtained from multiple CCF realisations. In the case of strongly correlated signals, values of $\tau_{\text{peak}}$ obtained from different CCF realisations will be nearly equal and close to the *assumed* true delay, thus resulting in a small ICS value. Conversely, large variability in the time delay estimates results in a large ICS value in the case of poorly correlated signals.

### 3.4. Workflow for assessing the quality of the time delay estimate

The steps for assessing the quality of the time delay estimate using the approaches described above can be summarised as follows:

1. Divide the measured signals into non-overlapping segments. Overlapping segments may result in correlated CCF peak values, distribution of which may not conform to either GEV or normal. For an accurate approximation of BIC, it is important to ensure that the number of segments is high (at least 30) [21].
2. Compute the CCF between corresponding segments of the two signals and determine the CCF peak value and time delay estimate in each CCF realisation.
3. Calculate the BIC (Eq. (11)) of the CCF peak values, assuming a type I GEV distribution ($M_1$) and a normal distribution ($M_2$), and then the BF ($\text{BF}_{M_1,M_2}$) using Eq. (10). Calculate the ICS using Eq. (19) and the PSR using Eq. (12) (or PMR using Eq. (16)). Note one may either evaluate the PSR or PMR value from the CCF of the whole signal or take the average of values obtained from different CCF realisations.
4. A high quality of the time delay estimate is inferred under the following conditions:
   (a) The BF $\text{BF}_{M_1,M_2}$ is less than 3.2. This suggests there is a lack of substantial evidence supporting the hypothesis that the signals are poorly correlated.
   (b) The PSR (PMR) is greater than the threshold $\lambda_{\text{PSR}}$ ($\lambda_{\text{PMR}}$) computed using Eq. (15) (Eq. (18)).
   (c) The ICS is less than some selected threshold $\lambda_{\text{ICS}}$. Based on simulation results, an inconsistency threshold of 1 is suggested. This value may, however, be adjusted if necessary, depending on the properties of the signals being considered.
   (d) The proportion of inconsistent estimates (PiCE) is less than some selected proportion, for example, 20%. This additional condition is included to avoid situations with a lot of outliers among the time delay estimates.

If any of these conditions is not satisfied, then low quality is inferred, and the time delay estimate is deemed inaccurate.

As already stated, poor correlation due to noise, interferences, and severe signal attenuation can result in reduced main peak, higher side lobe ('background' values), and appearance of additional peaks in the CCF. Each of the proposed indices may be more sensitive to some of these effects than others. For example, the PSR is sensitive to larger side lobe but less so to additional peaks that occur close to the main peak due to reflections in the measured signals [9]. Use of multiple indices based on different methodologies as proposed above will, therefore, be more robust for assessing the quality of time delay estimates than using a single index.

## 4. Results and discussion

In this section, the effectiveness of the proposed quality assessment indices is evaluated using experimental signals.

### 4.1. Comparative study of quality assessment indices

The performances of the existing and proposed alternative quality assessment indices were compared for datasets consisting of signals acquired on a laboratory leakage test rig. Fig. 4(a) shows the schematic of the rig, which consists of two 6-metre long MDPE pipes joined with a 90° elbow. Each pipe has with an outer diameter of 63 mm and thickness of 6.2 mm. Leaks can be simulated by opening valves installed on two 6-millimetre holes at the points marked L1 and L2 in the schematic (as shown in Fig. 4(b)). The rig is fitted with B200 hydrophones (https://www.neptune-sonar.co.uk/products/hydrophones/b200) and 352C22

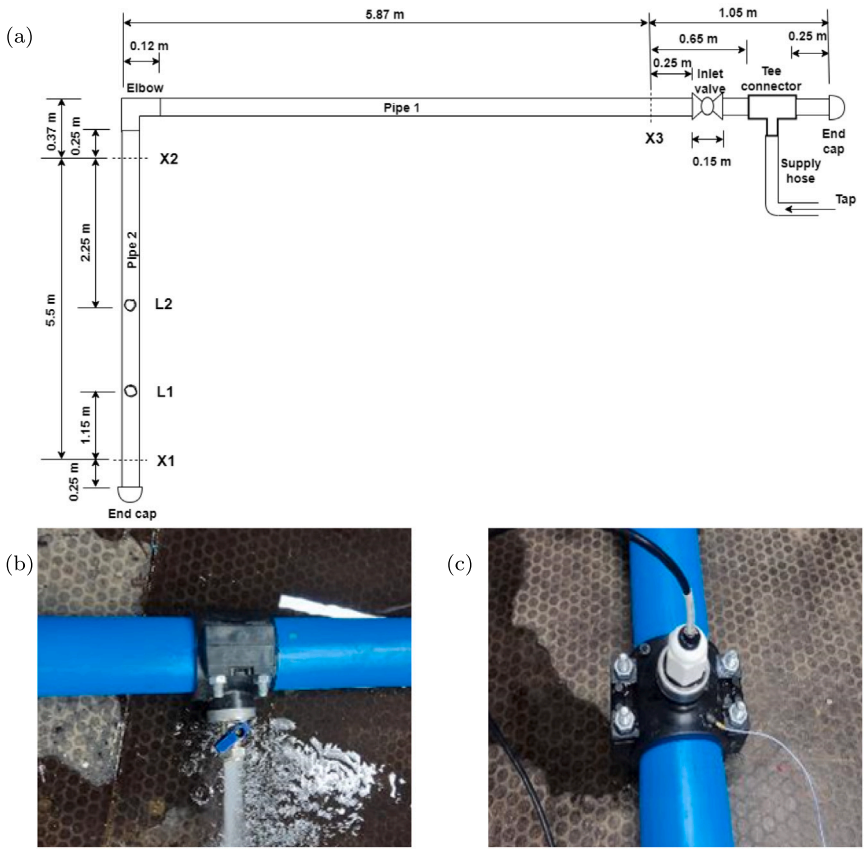


**Fig. 4.** Laboratory pipe leakage rig. (a) Schematic of the leakage rig. (b) Setup for leak simulation. (c) Access point for sensor installation.

**Table 2**
Metrological characteristics of the B200 hydrophone and 352C22 accelerometer.

| Sensor | B200 hydrophone | 352C22 accelerometer |
|---|---|---|
| Sensitivity | −212 dB re 1 V/mPa ($2.8 \times 10^{-5}$ mV/mPa) | 1.0 mV/(m $s^{-2}$) |
| Useful frequency range | 10 Hz to 180 kHz | 0.3 Hz to 20 kHz |
| Resonant frequency | 170 kHz | ≥50 kHz |
| Measurement range | Not available | ±4900 $ms^{-2}$ peak |
| Operating temperature | −5 to +40 °C | −54 to +121 °C |

accelerometers (https://www.pcb.com/it/products-it-it?model=352c22), the metrological characteristics of which are summarised in Table 2. These sensors are installed/mounted at the access points labelled X1, X2, and X3 as shown in Fig. 4(c). An additional accelerometer was mounted at a point located 2 m from X3 (this point will be denoted as X4). The acoustic wave speed in the MDPE pipe is 354 m/s (experimentally determined by exciting the pipe with a white noise signal using a shaker at the elbow and estimating the time delay between the pipe responses at X1 and X2). This value is the average of the wave speed values obtained for 10 hydrophone and accelerometer measurements.

Ten datasets consisting of leak signals acquired using hydrophones (4 datasets) or accelerometers (6 datasets) at the measurement points on the leakage test rig were analysed to evaluate the effectiveness of the quality assessment indices. The signals were measured at a sampling rate of 40 kHz for 30 s. Half of the hydrophone and accelerometer datasets were acquired in the presence of a leak at L1, while the rest were acquired when a leak was simulated at L2. For each dataset, the CCFs of the pairs of signals measured at points bracketing the leak (i.e., X1-X2, X1-X3, X1-X4) were computed with a maximum time lag of 8192 samples (205 ms). Prior to computing the CCF, the signals were first passed through a notch filter to remove any mains components, i.e., power-line frequency components, present in the signals. Mains components appear as spikes in the auto-power spectrum at 50 Hz and its harmonics. Each CCF of the leak signals is classified as either ‘high-quality’ or ‘low-quality’. A CCF is considered ‘high-quality’ if it is characterised by a prominent peak that gives an accurate time delay estimate. In this paper, a time delay estimate is considered accurate if it is within one time-domain delay resolution (inverse of the sampling frequency), i.e., 0.025 ms, from the true time delay. A CCF that

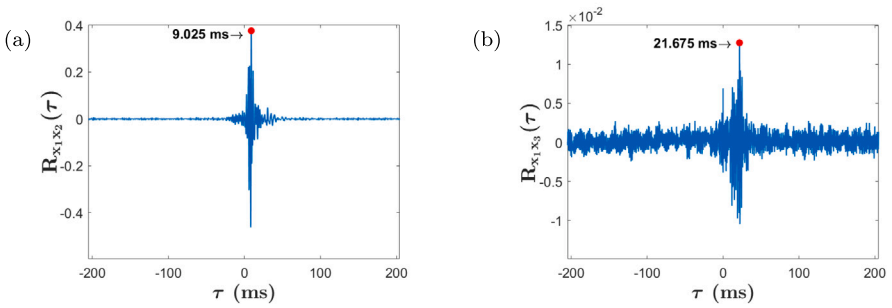


**Fig. 5.** Examples of CCFs obtained from accelerometer signals measured in the leakage rig in the presence of a leak at L1. (a) High-quality CCF of X1 and X2 signals. (b) Low-quality CCF of X1 and X3 signals.

**Table 3**
TDE quality assessment results for experimental leak signals. Yellow cells indicate positive inference about high quality (i.e., values that exceed, or in the case of the BF, ICS, and PiCE is less than, the quality assessment threshold).

| Index | Threshold | High-quality CCF | Low-quality CCF | Noise-only CCF |
|---|---|---|---|---|
| $\tau_{peak}$ (ms) | | 9.039 | 26.667 | – |
| $\tilde{\tau}_{peak}$ (ms) | | 9.025 | 21.675 | −103.7 |
| PiCE | 0.2 | 0.03 | 0.90 | 0.98 |
| ICS | 1.0 | 0.38 | 189 | 5854 |
| BF | 3.2 | 0.1 | 11.3 | 22.7 |
| PSR | 33.6 | 13 626 | 18.8 | 16.07 |
| PMR | 7.3 | 49.9 | 5.9 | 5.01 |
| BCFR | 0.3 | 0.54 | 0.38 | 0.053 |
| CQI | 0.2 | 0.45 | 0.42 | 0.17 |

**Table 4**
Average values of TDE quality indices for leak signals measured in the leakage test rig. Proportion of correct inferences are indicated in brackets.

| Index | Threshold | High quality | Low quality | Noise-only |
|---|---|---|---|---|
| PiCE | 0.2 | 0.03 | 0.79 | 0.97 |
| ICS | 1 | 0.55 (1.0) | 313.6 (0.89) | 3626 (1.0) |
| BF | 3.2 | 0.76 (0.94) | 5.5 (0.78) | 31.4 (1.0) |
| PSR | 33.6 | 9835 (1.0) | 28.7 (0.78) | 14.7 (1.0) |
| PMR | 7.3 | 33.4 (0.94) | 6.9 (0.78) | 4.9 (1.0) |
| BCFR | 0.3 | 0.69 (0.82) | 0.23 (0.22) | 0.036 (1.0) |
| CQI | 0.2 | 0.76 (0.88) | 0.34 (0.33) | 0.25 (1.0) |

does not give an accurate time delay estimate is considered 'low-quality' regardless of its shape. There are a total of 17 high-quality CCFs and 9 low-quality CCFs. An example of a high-quality CCF of signals measured at X1 and X2 is shown in Fig. 5(a), while Fig. 5(b) depicts a low-quality CCF calculated from signals acquired at X1 and X3.

Table 3 shows the values of the quality indices obtained for the high-quality and low-quality CCFs shown in Fig. 5 as well as the values for a pair of background noise signals measured at X1 and X2. The BF and ICS were calculated from the CCFs of 1-second signal segments, while the PSR and PMR were calculated from the CCF of the whole signal. The PSR and PMR thresholds were computed with an AFPR of 0.001. A time delay estimate is considered *consistent* if it differs from the *assumed* true delay by less than 2 samples (or 0.05 ms), and *inconsistent* otherwise. In the high-quality case, the *assumed* true delay is very close to the true delay, and all signal segments but one yield consistent estimates. In contrast, the *assumed* true delay differs substantially from the true delay in the low-quality and noise-only cases, and the high PiCE values indicate high variability in the estimates. The proposed quality assessment indices give inferences about the time delay estimate that are consistent with the quality of the CCFs in all three cases. While the BCFR and CQI give correct inferences in the high-quality and noise-only cases, they fail for the low-quality case.

The performance of the existing and alternative quality assessment indices were compared for all ten datasets. Table 4 presents the average values of the indices. The proportion of cases correctly identified by each index is indicated in brackets. The proposed indices achieve a higher true positive rate (TPR) and lower false positive rate (FPR) than the BCFR and CQI. Among all individual indices, the ICS achieves the best performance with the highest TPR of 100% and lowest FPR of 11%. The BF and PMR perform slightly worse than the PSR, achieving a TPR of 94% compared to 100% for the PSR.

As indicated by their relatively higher TPR and lower FPR, the proposed indices are more effective than the BCFR and CQI. Examining the two CCFs shown in Fig. 5 above reveals a possible reason for the bad performance of the CQI and the BCFR. Resonances and reflections present in the signals measured on the test rig manifest as additional peaks close to the main peak

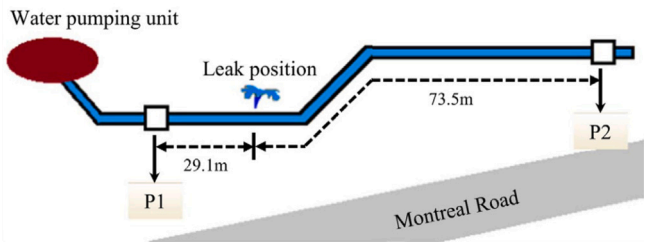


**Fig. 6.** Ottawa leakage test rig.

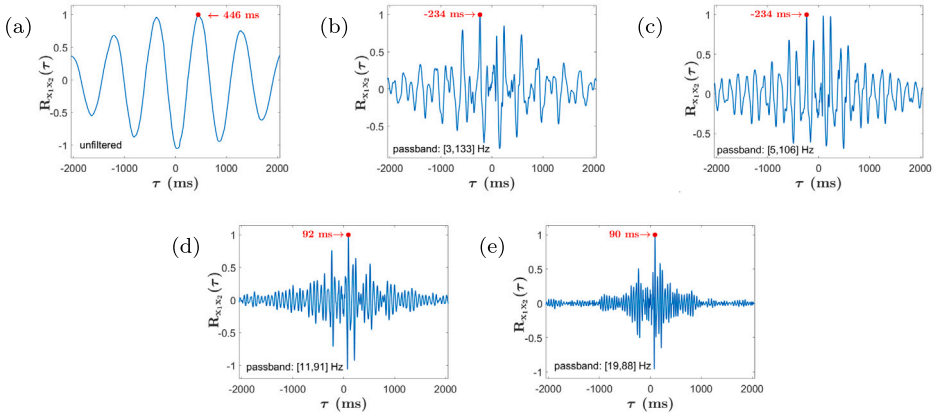


**Fig. 7.** CCFs of hydrophone leak signals. (a) Raw signals; (b) Filtered in the range [3, 133] Hz; (c) Filtered in the range [5, 106] Hz; (d) Filtered in the range [11, 91] Hz; (e) Filtered in the range [19, 88] Hz. Each CCF is normalised to its peak value.

in the CCF. As can be observed from Eqs. (3) and (4), reflection peaks immediately adjacent to the main CCF peak results in a low values for the BCFR and the bandwidth index even in CCFs with a 'good' shape, possibly leading to an incorrect inference. These additional peaks will also have more effect on the PMR than the PSR, as they will tend to increase the mean of the absolute values of the CCF, whereas they have no effect on the variance of the far points. The poor performances of the BCFR and CQI may also be related to the choice of their thresholds, which have been set heuristically without rigorous analysis. Refinement of the threshold selection methodology may improve their performance.

### *4.2. Selection of time delay estimation parameters using quality assessment indices*

The proposed quality assessment indices can be used to assess the effectiveness of available choices for TDE parameters, for example, filters. To illustrate their suitability for this purpose, the indices were applied to experimental signals acquired in a 200-metre long 150-millimetre diameter PVC pipe system located in a leakage test facility in Ottawa Canada, the schematic of which is shown in Fig. 6. A detailed description of the test site and measurement procedures has been given in [22]. Leak signals from a leaky joint in the buried pipe were measured using hydrophones installed on risers connected to two hydrants, one upstream and the other downstream of the joint. The distances between the leak and the measurement points were 32.8 m and 76.7 m (these distances include the lengths of the downstream and upstream risers: 3.7 m and 3.2 m, respectively). The signals were passed through an anti-aliasing filter with cut-off frequency set at 200 Hz and then sampled at 500 Hz. Hence, the time-domain resolution of the time delay estimate is 2 ms. Since the acoustic propagation speed in the PVC pipe was experimentally determined as 484 m/s [23], the true time delay is 90.7 ms.

To investigate the sensitivity of the proposed indices to changes in the quality of the time delay estimate, the signals were passed through different bandpass filters in order to obtain time delay estimates of different qualities. Fig. 7 shows the CCFs of the raw and filtered signals. Among these, only the CCFs of signals filtered in the frequency bands [11,91] (Fig. 7(d)) and [19,88] Hz (Fig. 7(e)) give accurate time delay estimates: 92 and 90 ms, respectively, which differ from the true delay by less than the time-domain resolution of 2 ms. These passbands fall within the frequency regions where the unwrapped cross-spectral phase (Fig. 8(a)) is approximately linear and the coherence (Fig. 8(b)) is high. This example illustrates the importance of properly selecting cut-off frequencies in correlation-based TDE methods.

Table 5 shows the values of the quality assessment indices obtained for raw and filtered signals. The BF and ICS were calculated from 1-second signal segments. Also shown in Table 5 are the time delay estimates $\hat{\tau}_{\text{peak}}$ obtained from the CCFs and the absolute

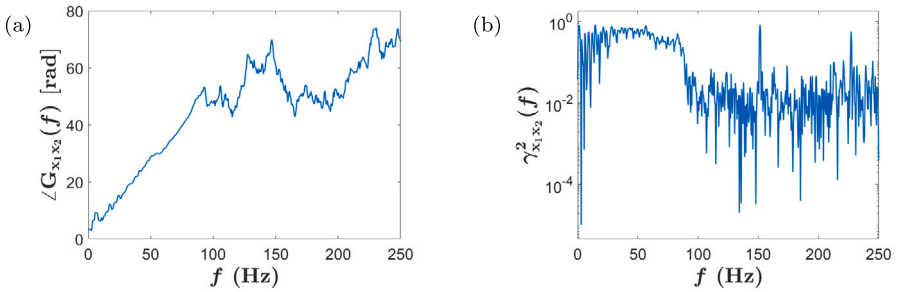


**Fig. 8.** Spectral analysis of raw hydrophone signals. (a) Unwrapped cross-spectral phase; (b) Magnitude-squared coherence.

**Table 5**
TDE quality assessment results for raw and filtered experimental leak signals. Yellow cells indicate positive inference about high quality.

| $\tau_{peak}$ (ms) | | 90.7 | | | | |
|---|---|---|---|---|---|---|
| Passband (Hz) | | Raw | [3,133] | [5,106] | [11,91] | [19,88] |
| $\hat{\tau}_{peak}$ (ms) | | 444 | 232 | 232 | 92 | 90 |
| $\Delta d_1$ (m) | | 85.5 | 34.2 | 34.2 | 0.31 | 0.17 |
| Index | Threshold | | | | | |
| $\tilde{\tau}_{peak}$ (ms) | | 446 | 232 | 232 | 92 | 90 |
| PiCE | 0.2 | 0.93 | 0.78 | 0.73 | 0.11 | 0.07 |
| ICS | 1 | 51.5 | 37.6 | 14.4 | 0.68 | 0.28 |
| BF | 3.2 | $9.91 \cdot 10^{15}$ | 21.8 | 118 | 0.52 | 0.29 |
| PSR | 33.6 | 3.31 | 18.6 | 20.7 | 73.8 | 339 |
| PMR | 7.3 | 1.85 | 4.59 | 4.75 | 7.53 | 13 |

error in the leak location $\Delta d_1$. The values of the proposed indices are consistent with the quality of the time delay estimate. The large relative difference in the values of the indices for the low-quality and high-quality cases shows that they are adequate for assessing the effectiveness of available TDE parameters. The PSR and PMR are especially practically convenient for this application, since they can be calculated from a single CCF realisation.

Based on the experimental results presented in this section, the proposed quality assessment indices, namely BF, PSR, PMR, and ICS, can discriminate between low-quality and high-quality time delay estimates. Thus, they present an effective means to objectively assess the reliability of TDE results. However, it is important to note that their effectiveness may reduce in the absence of a leak but presence of correlated background noise, since their use is based on the assumption that 'low-quality' CCFs only result from poorly correlated signals. Development of means to check for the presence of correlated background noise when assessing the quality of the time delay estimate will be considered in a future study. Further experimental validation of the indices in different measurement environments is highly recommended.

## 5. Conclusion

In this paper, three approaches were developed for assessing the quality of the time delay estimate by considering the statistical properties of the cross-correlation function (CCF). The information criterion approach uses the Bayesian Factor (BF) to assess the probability distribution of the CCF peak values. In the processing gain approach, two indices, the peak-to-side ratio (PSR) and the peak-to-mean ratio (PMR) are employed to describe the detectability of the CCF peak relative to other values in the CCF. The statistical approach assesses the accuracy of the time delay between signals based on an index termed the inconsistency score (ICS), which is defined as the root-mean square of deviations of time delay estimates from their statistical mode. Experimental results demonstrate that the proposed indices are more effective in correctly inferring the quality of the time delay estimate compared to existing indices available in the literature. They also present viable means of selecting the best available parameters in correlation-based time delay estimation (TDE) methods, for example, the cut-off frequencies of the applied filters.

## CRediT authorship contribution statement

**Ndubuisi Uchendu:** Writing – review & editing, Writing – original draft, Validation, Investigation. **Jennifer M. Muggleton:** Writing – review & editing, Supervision, Project administration, Funding acquisition, Conceptualization, Methodology. **Paul R. White:** Writing – review & editing, Supervision, Project administration, Methodology.

## Declaration of competing interest

The authors declare that they have no known competing financial interests or personal relationships that could have appeared to influence the work reported in this paper.

## Acknowledgements

The authors would like to thank Centre for Doctoral Training Sustainable Infrastructure Systems (CDT-SIS) University of Southampton, United Kingdom Water Industry Research (UKWIR), and Petroleum Technology Development Fund (PTDF) Nigeria for sponsoring this project.

## Appendix. Expression for the peak-to-side lobe ratio of leak signals

If the leak noise spectrum $G_{ll}(\omega)$ is assumed to be flat with power spectral density $S_0$, the expected value of the CCF peak $R_{\max} = R_{x_1x_2}(\tau_{\text{peak}})$ is given by

$$\mathrm{E}\{R_{\max}\} = R_{l_1l_2}(\tau_{\text{peak}}) = \frac{S_0}{\pi\beta d} \tag{A.1}$$

where $R_{l_1l_2}(\tau) = \mathcal{F}^{-1}\left\{G_{l_1l_2}(\omega)\right\} = \mathcal{F}^{-1}\left\{G_{ll}(\omega)\exp(-|\omega|\beta d)\exp(-\mathrm{j}\omega\tau_{\text{peak}})\right\}$ is the biased CCF of the noise-free components of measured leak signals (i.e., the first term in Eq. (5)), and $S_0$ is the power spectral density of the leak noise which has been assumed to be flat, i.e., $G_{ll}(\omega) = S_0$. For a long measurement time $T$, the variance of the cross-correlation value at an arbitrary lag $\tau$ is given by [24]

$$\mathrm{var}\{R_{x_1x_2}(\tau)\} \approx \frac{1}{T}\int_{-\infty}^{\infty}\left(R_{x_1x_1}(\zeta)R_{x_2x_2}(\zeta) + R_{x_1x_2}(\zeta+\tau)R_{x_1x_2}(\zeta-\tau)\right)d\zeta. \tag{A.2}$$

The cross-correlation values of bandlimited signals approaches zero at lags $\tau$ much greater than the correlation time of the signals, which implies that $R_{x_1x_1}(\zeta)R_{x_2x_2}(\zeta) \gg R_{x_1x_2}(\zeta+\tau)R_{x_2x_1}(\zeta-\tau)$ for $\tau \gg 0$ [24]. Thus, since the leak noise and the background noise signals are assumed to be uncorrelated, the variance at $\tau_{\text{far}} \gg \tau_{\text{peak}}$ can be approximated as

$$\begin{aligned}\mathrm{var}\{R_{x_1x_2}(\tau_{\text{far}})\} \approx& \frac{1}{T}\int_{-\infty}^{\infty}\begin{pmatrix}R_{l_1l_1}(\zeta)R_{l_2l_2}(\zeta) + R_{l_1l_1}(\zeta)R_{n_2n_2}(\zeta)\\ + R_{n_1n_1}(\zeta)R_{l_2l_2}(\zeta) + R_{n_1n_1}(\zeta)R_{n_2n_2}(\zeta)\end{pmatrix}d\zeta\\ =& \frac{1}{2\pi T}\int_{-\infty}^{\infty}\begin{pmatrix}G_{l_1l_1}(\omega)G_{l_2l_2}(\omega) + G_{l_1l_1}(\omega)G_{n_2n_2}(\omega)\\ + G_{n_1n_1}(\omega)G_{l_2l_2}(\omega) + G_{n_1n_1}(\omega)G_{n_2n_2}(\omega)\end{pmatrix}d\omega\end{aligned} \tag{A.3}$$

where the last equality follows from Parseval's theorem. Rewriting the auto-power spectra $G_{l_1l_1}(\omega)$ and $G_{l_2l_2}(\omega)$ in terms of the pipe FRF (Eq. (6)) and assuming flat spectra $G_{n_1n_1}(\omega) = G_{n_2n_2}(\omega) = N_0$ for the background noise signals in the analysed frequency region $\omega_1 \le \omega \le \omega_2$ with $\omega_2 \gg \omega_1$, this equation is expressed as

$$\mathrm{var}\{R_{x_1x_2}(\tau_{\text{far}})\} \approx \frac{1}{\pi T}S_0^2\left(\begin{array}{l}\dfrac{1}{2\beta d}\exp(-2\omega_1\beta d)\displaystyle\sum_{k=0}^{2}\frac{(2\omega_1\beta d)^k}{k!} + \frac{N_0}{S_0}\frac{1}{2\beta d_1}\exp(-2\omega_1\beta d_1)\sum_{k=0}^{2}\frac{(2\omega_1\beta d_1)^k}{k!}\\ +\dfrac{N_0}{S_0}\dfrac{1}{2\beta d_2}\exp(-2\omega_1\beta d_2)\displaystyle\sum_{k=0}^{2}\frac{(2\omega_1\beta d_2)^k}{k!} + \frac{N_0^2}{S_0^2}\omega_2\end{array}\right). \tag{A.4}$$

The integrals have been evaluated using the relation [25]

$$\int_0^b \omega^n\exp(-a\omega)d\omega = \frac{n!}{a^{n+1}}\left[1-\exp(-ab)\sum_{k=0}^{n}\frac{(ab)^k}{k!}\right], \ldots, a > 0. \tag{A.5}$$

Hence, the PSR is obtained as

$$\begin{aligned}\mathrm{PSR} =& \frac{\left(\mathrm{E}\{R_{\max}\}\right)^2}{\mathrm{var}\{R_{x_1x_2}(\tau_{\text{far}})\}}\\ =& \frac{T}{\pi(\beta d)^2}\left(\begin{array}{l}\dfrac{1}{2\beta d}\exp(-2\omega_1\beta d)\displaystyle\sum_{k=0}^{2}\frac{(2\omega_1\beta d)^k}{k!} + \frac{N_0}{S_0}\frac{1}{2\beta d_1}\exp(-2\omega_1\beta d_1)\sum_{k=0}^{2}\frac{(2\omega_1\beta d_1)^k}{k!}\\ +\dfrac{N_0}{S_0}\dfrac{1}{2\beta d_2}\exp(-2\omega_1\beta d_2)\displaystyle\sum_{k=0}^{2}\frac{(2\omega_1\beta d_2)^k}{k!} + \frac{N_0^2}{S_0^2}\omega_2\end{array}\right)^{-1}.\end{aligned} \tag{A.6}$$

## Data availability

Data will be made available on request.

## References


[1] R. Cramer, D. Shaw, R. Tulalian, P. Angelo, M. van Stuijvenberg, Detecting and correcting pipeline leaks before they become a big problem, Mar. Technol. Soc. J. 49 (1) (2015) 31–46, http://dx.doi.org/10.4031/mtsj.49.1.1.

[2] D. Rogers, Leaking water networks: An economic and environmental disaster, Procedia Eng. 70 (2014) 1421–1429, http://dx.doi.org/10.1016/j.proeng.2014.02.157.

[3] UNESCO, The United Nations World Water Development Report 2023: Partnerships and Cooperation for Water, UNESCO World Water Assessment Programme, 2023, p. 189, https://unesdoc.unesco.org/notice?id=p::usmarcdef_0000384655.

[4] Z. Liu, Y. Kleiner, B. Rajani, L. Wang, W. Condit, Condition Assessment Technologies for Water Transmission and Distribution Systems, vol. EPA/600/R-12/017, EPA, USA, 2012.

[5] M.J. Brennan, D.N. Chapman, P.F. Joseph, N. Metje, J.M. Muggleton, E. Rustighi, Achieving Zero Leakage by 2050: Detection and Location Methods Acoustic Leak Detection, UK Water Industry Research (UKWIR), London, United Kingdom, 2017, https://ukwir.org/achieving-zero-leakage-by-2050-leakage-detection-by-acoustic-methods-1.

[6] F.C.L. Almeida, Improved Acoustic Methods for Leak Detection in Buried Plastic Water Distribution Pipes (Ph.D. thesis), University of Southampton, 2013, https://eprints.soton.ac.uk/355964/.

[7] P.C. Ayala Castillo, An Investigation into Some Signal Processing Techniques for the Development of a Low-Cost Acoustic Correlator to Detect and Locate Leaks in Buried Water Pipes (Ph.D. thesis), São Paulo State University, 2019, https://repositorio.unesp.br/server/api/core/bitstreams/60873347-78fc-4899-8a09-98ea3f751172/content.

[8] F.C.L. Almeida, M.J. Brennan, P.F. Joseph, Y. Gao, A.T. Paschoalini, The effects of resonances on time delay estimation for water leak detection in plastic pipes, J. Sound Vib. 420 (2018) 315–329, http://dx.doi.org/10.1016/j.jsv.2017.06.025.

[9] Y. Gao, Leak Detection in Plastic Water Pipes (Ph.D. thesis), University of Southampton, 2006, https://eprints.soton.ac.uk/465828/.

[10] C. Knapp, G. Carter, The generalized correlation method for estimation of time delay, IEEE Trans. Acoust. Speech Signal Process. 24 (4) (1976) 320–327, http://dx.doi.org/10.1109/tassp.1976.1162830.

[11] G. Roe, G. White, Probability density functions for correlators with noisy reference signals, IRE Trans. Inf. Theory 7 (1) (1961) 13–18, http://dx.doi.org/10.1109/TIT.1961.1057613.

[12] J.A. Hanson, H. Yang, Quantitative evaluation of cross correlation between two finite-length time series with applications to single-molecule FRET, J. Phys. Chem. B 112 (44) (2008) 13962–13970, http://dx.doi.org/10.1021/jp804440y.

[13] S. Kotz, S. Nadarajah, Extreme Value Distributions: Theory and Applications, Imperial College Press, London, UK, 2000, p. 185, http://dx.doi.org/10.1142/p191.

[14] H. Jeffreys, The Theory of Probability, third ed., Clarendon Press, Oxford, UK, 1998.

[15] J. Gill, Bayesian hypothesis testing and the Bayes factor, in: Bayesian Methods: A Social and Behavioral Sciences Approach, Chapman and Hall, 2002, pp. 199–237, http://dx.doi.org/10.1201/b17888.

[16] E.-J. Wagenmakers, T. Lodewyckx, H. Kuriyal, R. Grasman, Bayesian hypothesis testing for psychologists: A tutorial on the Savage–Dickey method, Cogn. Psychol. 60 (3) (2010) 158–189, http://dx.doi.org/10.1016/j.cogpsych.2009.12.001.

[17] G. Schwarz, Estimating the dimension of a model, Ann. Statist. 6 (2) (1978) 461–464, 4, http://dx.doi.org/10.1214/aos/1176344136.

[18] R.E. Kass, A.E. Raftery, Bayes factors, J. Amer. Statist. Assoc. 90 (430) (1995) 773–795, http://dx.doi.org/10.1080/01621459.1995.10476572.

[19] D. Casasent, G. Silbershatz, B.V.K. Vijaya Kumar, Acoustooptic matched filter correlator, Appl. Opt. 21 (13) (1982) 2356–2364, http://dx.doi.org/10.1364/AO.21.002356.

[20] K. Cooray, M. Ananda, A generalization of the half-normal distribution with applications to lifetime data, Comm. Statist. Theory Methods 37 (2008) 1323–1337, http://dx.doi.org/10.1080/03610920701826088.

[21] J. Lorah, A. Womack, Value of sample size for computation of the Bayesian information criterion (BIC) in multilevel modeling, Behav. Res. Methods 51 (1) (2019) 440–450, http://dx.doi.org/10.3758/s13428-018-1188-3.

[22] O. Hunaidi, W. Chu, A. Wang, W. Guan, Detecting leaks in plastic pipes, J. Am. Water Works Assoc. 92 (2) (2000) 82–94, http://dx.doi.org/10.1002/j.1551-8833.2000.tb08819.x.

[23] Y. Gao, M.J. Brennan, P.F. Joseph, A comparison of time delay estimators for the detection of leak noise signals in plastic water distribution pipes, J. Sound Vib. 292 (3–5) (2006) 552–570, http://dx.doi.org/10.1016/j.jsv.2005.08.014.

[24] J.S. Bendat, A.G. Piersol, Random Data, in: Wiley Series in Probability and Statistics, Wiley, 2010.

[25] I. Gradshteyn, I. Ryzhik, Table of Integrals, Series, and Products, seventh ed., Academic Press, USA, 2007.